



# **STUDY ON BEHAVIOUR OF COLD FORMED BUILT-UP I-SECTION WITH TRAPEZOIDAL CORRUGATION IN WEB BY VARYING THE ASPECT RATIO AND ANGLE OF CORRUGATION**

**V. C. PRABHA<sup>\*</sup>, A. SHALINI, S. SARAVANAGANESH and  
K. SELVAKUMAR**

Department of Civil Engineering, K. S. R College of Engineering,  
TIRUCHENGODE (T.N.) INDIA

## **ABSTRACT**

The use of cold-formed steel structures is increasing throughout the world as they are efficient in terms of stiffness and strength. Structural instability of the section is more likely to occur. To improve their strength and to eliminate local buckling of web elements, trapezoidal corrugated web is used. There are totally 8 beams in that; the four trial beam having aspect ratio varies from 0.5, 1, 1.5, and 2. The another four trial beam having angle of corrugation varies from 15°, 30°, 45°, 60° and the other parameters such as length of span (3000 mm), flange width (100 mm), thickness of flange (2 mm), thickness of web (1.2 mm), lip size (15 mm) and depth of web (300) are constant for all the eight trial beams. Four beams were fabricated and experimented under two point loading. A tension test was done for three series of specimens with 2 mm thickness to determine the Young's modulus and yield stress. It was observed that the load carrying capacity of AR2 having aspect ratio 1 and DC3 angle of corrugation 45° specimen's increases more, when compared to other specimens and it also reaches maximum deflection, which does not undergo any major failure. Hence, the cold-formed steel section with trapezoidal corrugated web beams can be applicable in structural components.

**Key words:** Cold formed 'I' section, Aspect ratio, Angle of corrugation, Trapezoidal corrugation.

## **INTRODUCTION**

Nowadays, a multiplicity of widely different products, with a tremendous diversity of shapes, sizes, and applications are produced in steel using the cold forming process. The use of cold-formed steel members in building construction began in about the 1850s in both

---

<sup>\*</sup> Author for correspondence; E-mail: prabhacsamy@gmail.com, Mo.: +91-9566340507  
shalini.me19@yahoo.com, Mo.: +91-9566979787

the United States and U.K. However, such steel members were not widely used in buildings until 1940<sup>1-3</sup>. In the recent years, it has been recognized that cold-formed steel sections can be used effectively as primary framing components. Cold-formed steel in the form of profiled decking has gained widespread acceptance over the past fifteen years as a basic component, along with concrete, in composite slabs. Cold-formed steel members are efficient in terms of both their stiffness and strength<sup>4</sup>. In addition, because the steel may be even less than 1 mm thick, the members are light weight. The already impressive load carrying capabilities of cold-formed steel members will be enhanced by current work to develop composite systems, both for wall and floor structures. The use of cold-formed steel structures is increasing throughout the world with the production of more economic steel coils particularly in coated form with zinc or aluminum/zinc coatings. These coils are subsequently formed into thin-walled sections by the cold-forming process.

They are commonly called “Light gauge sections” since their thickness has been normally less than 3 mm. However, more recent developments have allowed sections up to 25 mm to be cold-formed, and open sections up to approximately 8 mm thick are becoming common in building construction. The steel used for these sections may have a yield stress ranging from 250 M<sub>Pa</sub> to 550 M<sub>Pa</sub><sup>5</sup> (Hancock, 1997). The use of thinner sections and high strength steels leads to design problems for structural engineers, which may not normally be encountered in routine structural steel design. Structural instability of the sections is more likely to occur as a result of the reduced buckling loads (and stresses), and the use of higher strength steel, which may make the buckling stress and yield stress of the thin-walled sections approximately equal. Further, the shapes, which can be cold-formed are often considerably more complex than hot-rolled steel shapes such as I-sections and unlipped channel sections<sup>6,7</sup>. The cold-formed sections commonly have mono-symmetric or point symmetric shapes, and normally have stiffening lips on flanges and intermediate stiffeners in wide flanges and webs. Both simple and complex shapes can be formed for structural and non-structural applications. Special design standards have been developed for these sections.

The range of use of cold-formed steel sections specifically as load-bearing structural components is very wide, taking in the Automobile industry, Ship building, Rail transport, the Aircraft industry, Highway engineering, Agricultural and Industry equipment, Office equipment, Chemical, Mining, Petroleum, Nuclear and Space industries. In building construction, cold-formed steel products are mainly used as structural members, diaphragms and coverings for roofs, wall, and floors. Some of these advantages are:

- As compared with thicker hot-rolled shapes, cold-formed light members can be manufactured for relatively light loads and short spans.
- Nest able sections can be produced, allowing for compact packaging and shipping.
- Freedom from corrosion, in internal environments.
- Unusual sectional configurations can be produced economically by cold-forming operations and consequently favorable strength-to-weight ratios can be obtained.
- Recycled and recyclable material.
- Lintels over door and window openings in masonry construction.
- Cross sectional shapes are formed to close tolerances and these can be consistently repeated for as long as required.
- They are usually light making it easy to transport and erect.
- Storage racking.
- Coefficient of thermal expansion comparable with that of concrete.

The main objective of the present research is to investigate the behavior of cold-formed corrugated I beam with varying the aspect ratio ( $a/b$ ) and depth of trapezoidal corrugation subjected to two point load. The results are experimentally tested and compared with theoretical data's as per North American Specification standards (NAS – 2001) and possible modes of failures in beams are studied.

## **EXPERIMENTAL**

### **Tensile test on steel sheet**

A model of cold-formed sheets of 2 mm thickness are used to fabricate flange of the lipped I-section, 1.2 mm for the web as per IS 1663-1960 part I as shown in Fig. 1. A 3 mm thick plate is used as stiffener under the loading points (i.e.  $L/3$  span) and at the supports to avoid bearing failure. Totally three specimens were fabricated for the above-mentioned dimensions to find the Young's modulus and yield stress by conducting the tensile test in a universal testing machine. From the plotted graphs, average yield stress and Young's modulus value are given in Table 1<sup>8</sup>.

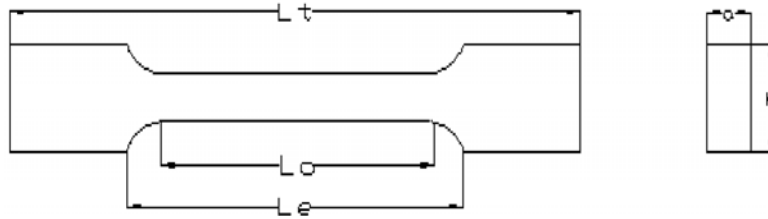


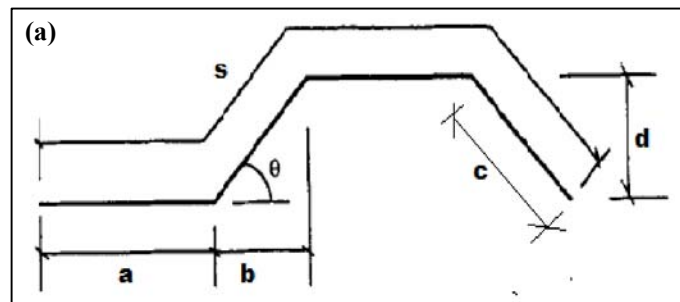
**Fig. 1: Tensile test-steel sheet specimen**

**Table 1: Tensile test result on steel sheet**

Specimen details	F <sub>y</sub>	Young's modulus (N/mm <sup>2</sup> )	Yield stress (N/mm <sup>2</sup> )
Model 1	210	$1.96 \times 10^5$	210
Model 2	205	$1.87 \times 10^5$	205
Model 3	220	$2.15 \times 10^5$	220
<b>Average</b>		<b><math>1.99 \times 10^5</math></b>	<b>211.67</b>

### Details of the specimens

From eight specimens, four beams, with varying aspect ratio of 1:0.5, 1:1, 1:1.5 and 1:2, namely AR1, AR2, AR3 and AR4 and, four specimens with varying angle of corrugation DC1, DC2, DC3 and DC4 were tested with flange width of 100 mm, lip size 15 mm, and the flange thickness is 2 mm. The height and thickness of the web are 300 mm and 1.2 mm, respectively. Four stiffeners of 3 mm were used in each beam and stiffeners were located exactly at the position where the loads and support reactions were applied. The spans of all beams were 3000 mm<sup>9</sup>. The detailed nominal dimensions of the specimens are shown in Fig. 2 and Table 2.



Cont...

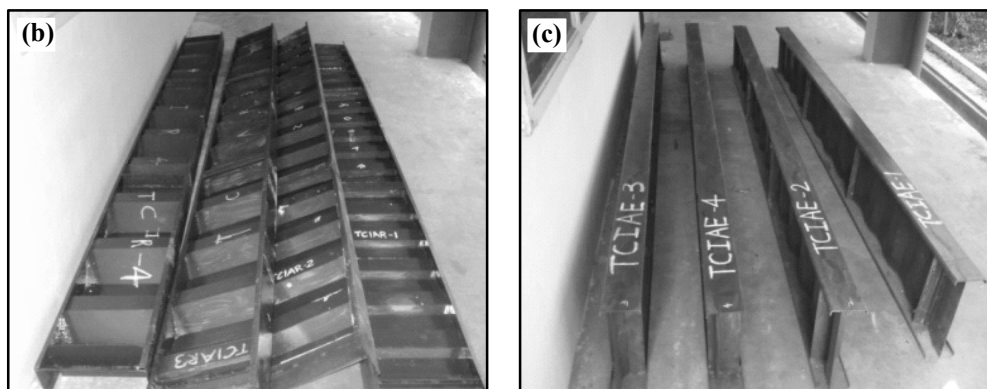


**Fig. 2(a): Corrugation configuration parameters (b) Varying aspect ratio (c) Varying angle of corrugation**

**Table 2: Detailed corrugation configurations**

Specimen ID	Corrugation configurations						Aspect ratio ( $\beta = a/c$ )
	a	c	b	s	d	$\theta^\circ$	
AR-1	60	28.3	20	176.6	20	45	0.5
AR-2	60	60	40	240	40	45	1
AR-3	60	84.85	60	289.7	60	45	1.5
AR-4	60	113.1	80	346.2	80	45	2
DC1	60	60	57.95	240	15.53	15	1
DC2	60	60	51.9	240	30.00	30	1
DC3	60	60	42.42	240	42.42	45	1
DC4	60	60	30	240	51.90	60	1

### Experimental test setup

A 50T capacity self-straining loading frame is used to conduct the experiment for all specimens. A load cell with the capacity of 100 kN was used to monitor the load. Each specimen was simply supported at both ends and loaded at  $L/3$  and  $2L/3$  of the span. A clamping arrangement is used to arrest the lateral rotation of specimen during testing. The test setup of the specimen is shown in Figs. 3 and 4, which is same for all the specimens. The beams were instrumented using three LVDTs under the mid-span,  $L/3$  of span, and lip of mid span top flange<sup>10</sup>. Three-strain gauges were attached to the specimens one in web at

300 mm from support of beam, second in middle of bottom tension flange, third strain gauge in middle top compression flange of beams and the data were collected by using Data Acquisition System. A loading set up is shown in Fig. 3.



**Fig. 3: Experimental test set up**

### Experimental results of specimens

#### Load carrying capacity of beams

By varying the aspect ratio in beam, the specimen was loaded gradually up to failure, and the beam failed between 38.74 kN to 43.63 kN, in AR1, AR2, AR3 and AR4 beam. By varying the depth of corrugation, the beam failed between 39.8 kN to 43.63 kN. The failure modes were taken in beam as lateral torsional buckling, crushing of compression flange, and bearing the failure. Initiation of local buckling has taken place at the load of 34.76 kN and then failure of flange of AR1 beam at 36.62 kN. Similarly, for AR3 specimen, the buckling was initiated at 35.36 kN. By keeping aspect ratio 1, the section undergoes maximum load carrying capacity of 43.63 kN.



**Fig. 4 (a): Lateral torsional buckling (b) Bearing failure**

The critical load for DC3 i.e. (angle of corrugation 45<sup>0</sup>) wasure identified only at 34.77 kN, which is more, when compared to other three set of specimens. The failure mode of the specimen is shown in Fig. 4. The experimental test results are charted in Fig. 5. The failure mode of beams is mentioned in Table 3.

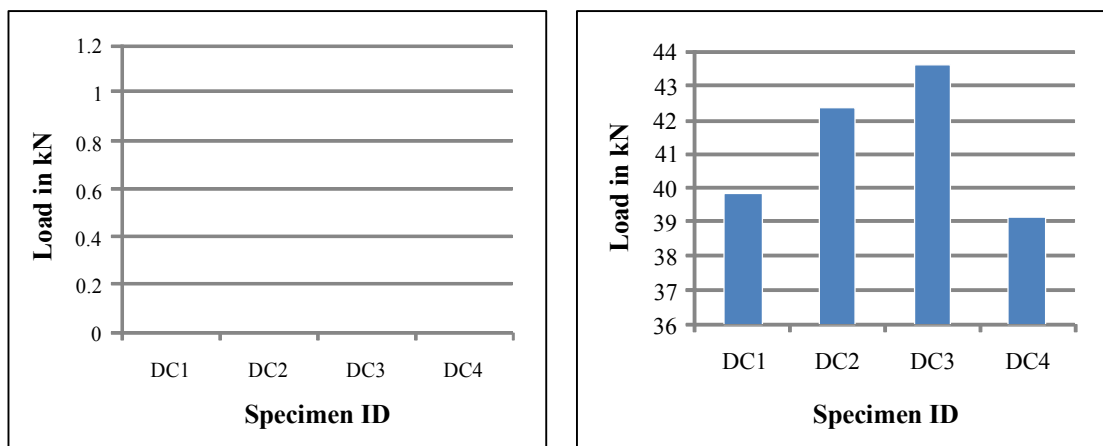


**Fig. 5: Load carrying capacity of beam by varying aspect ratio and angle of corrugation**

**Table 3: Failure mode of beams**

Specimen name								
Specimen ID	AR 1	AR 2	AR 3	AR 4	DC 1	DC 2	DC 3	DC 4
Failure mode	Lateral torsional buckling	Lateral torsional buckling	Bearing failure	Lateral buckling	Lateral buckling	Lateral torsional buckling	Bearing failure	Lateral torsional buckling

**Load-deflection curve of beams**

From LVDT, the deflection at mid-span & @ L/3 distance is noted. The lateral deflection is identified at mid-span of top compression flange lip of beams. The graphs for load Vs deflection and load Vs strain were plotted for all the specimens and are shown in Figs. 6 to 11. From the graphs of the specimens, when aspect ratio  $\beta=a/c =1$  and the angle of corrugation 45 degrees, it has been observed that the specimen has the maximum load carrying capacity.

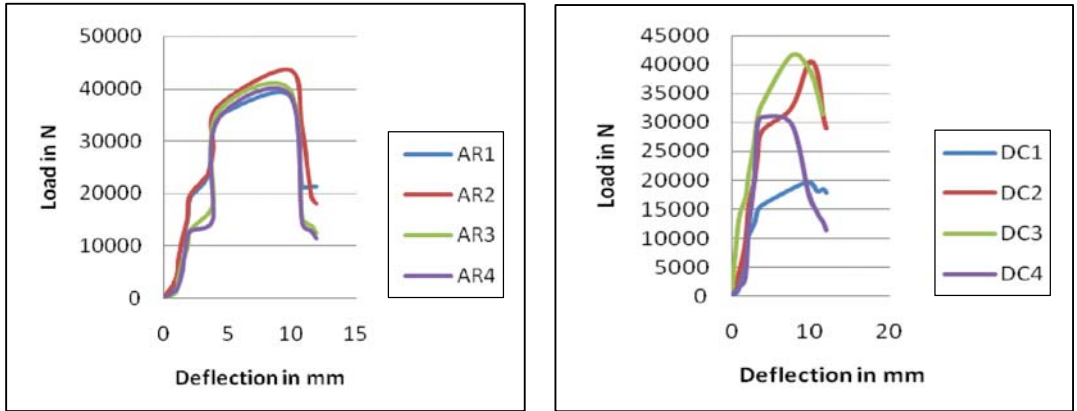


**Fig. 6: Load Vs Deflection @ mid span of beams**

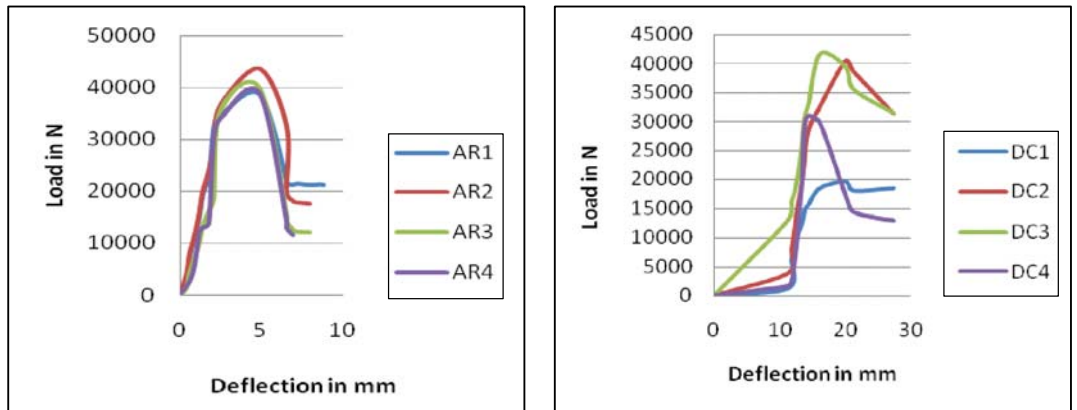


**Fig. 7: Load Vs Deflection @ L/3 span of beams**

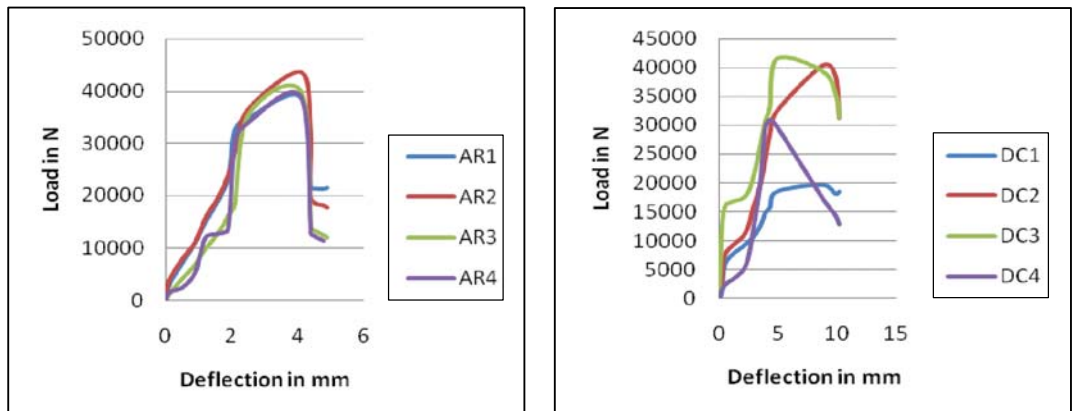


**Fig. 8: Load Vs Lateral deflection at mid span in top compression flange lip of beams**

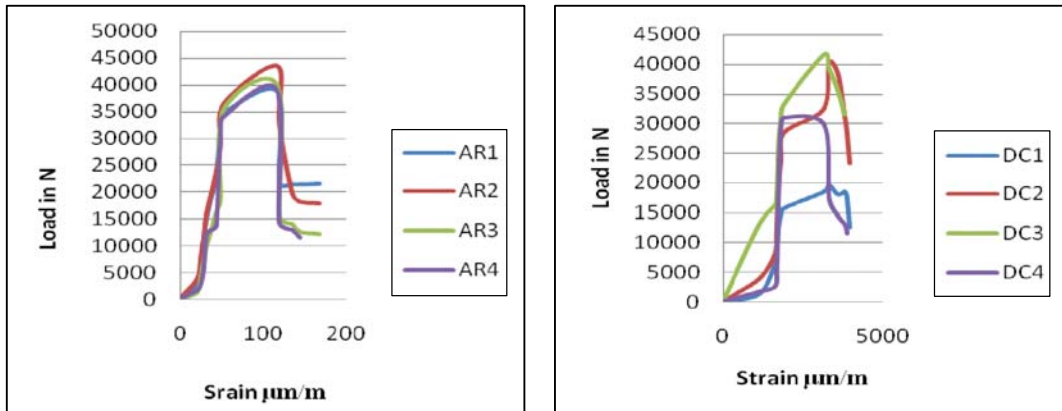


Fig. 9: Load Vs Strain in web at 300 mm from support of beams

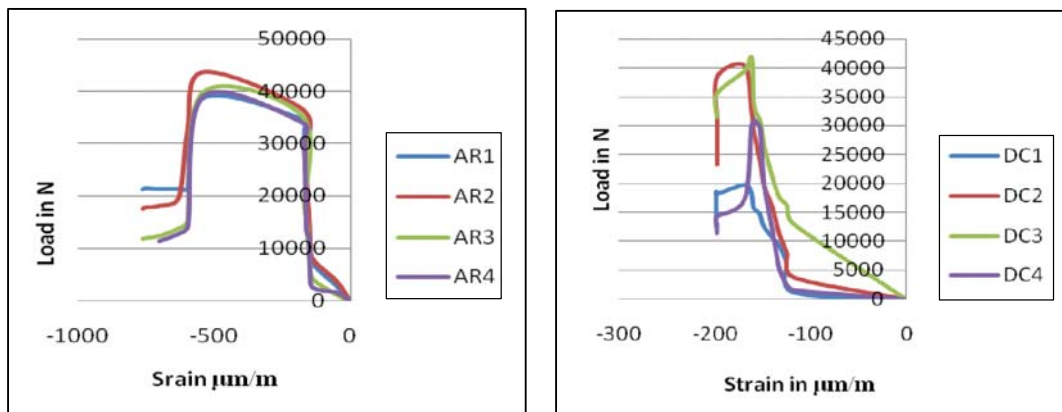


Fig. 10: Load Vs Strain in middle of bottom tension flange of beams

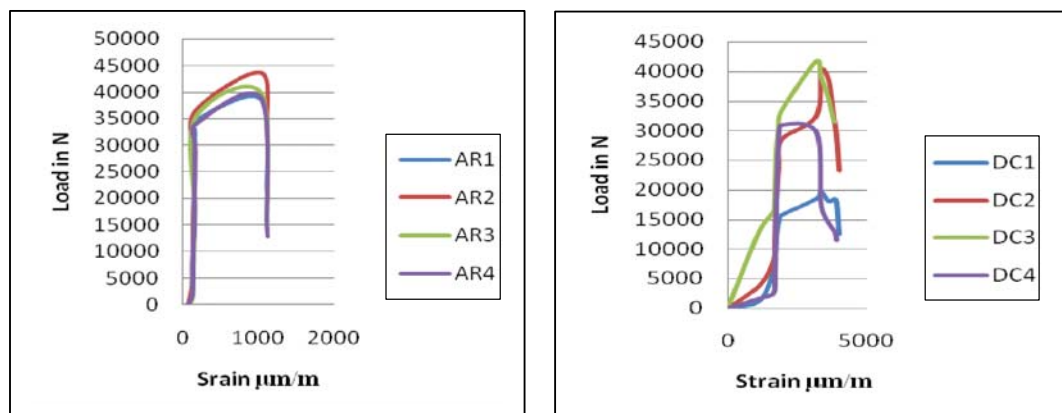


Fig. 11: Load Vs Strain at middle top compression flange of beams

From the load deflection curves of specimens, varying aspect ratio, AR1, AR2, AR3, AR4; the specimen AR2 having aspect ratio 1 has 19% more load carrying capacity than the other three. In the specimens varying corrugation angle, DC1, DC2, DC3, DC4, the load carrying capacity for maximum deflection is maximum for DC3. The ultimate load varied by 3% for DC2 (Corrugation angle 30°) and DC3 (Corrugation angle 45°).

## RESULTS AND DISCUSSION

### General

The load carrying capacities of specimens, estimated by using North American Specification Standards, theoretical analysis has been compared with the Numerical Analysis and experimental failure load. Discussions were carried out with respect to the load carrying capacities and the failure mode occurred.

**Table 6.1: Comparison of load**

Specimen name	Aspect ratio	Experimental results, load in (kN)	
		Critical load	Ultimate load
AR 1	0.5	32.76	38.74
AR 2	1	34.51	43.63
AR 3	1.5	33.32	39.87
AR 4	2	32.97	38.99
DC1	15°	31.92	39.80
DC2	30°	32.84	42.39
DC3	45°	34.77	43.63
DC4	60°	33.88	39.10

## CONCLUSION

An experimental investigation into the behavior of cold-formed steel beam I section with corrugated web with two point loading is described in this paper.

The following conclusions can be made from the experimental test results.

- (i) From the above table of the experimental results, when the aspect ratio increases, the load carrying capacity of the specimen increases. When the aspect ratio is 1, the load carrying capacity is maximum.
- (ii) From the experimental results, it is observed that as the angle of corrugation increases, the load carrying capacity increases. Experimental analysis- the load carrying capacity is maximum, when the corrugation angle is 45°.
- (iii) All the specimens fail due to lateral torsion buckling. Failure in the web is eliminated due to provision of corrugation in web.
- (iv) Bearing failure is eliminated due to the provision of stiffeners at the loading points (L/3, 2L/3) and supports.

## **REFERENCES**

1. A. Romeijn, R. Sarkhosh and Huigert de Hoop, Basic Parametric Study on Corrugated Web Girders with Cut Outs, *J. Constructional Steel Res.*, **65**, 395-407 (2009).
2. E. Y. Sayed-Ahmed, Design Aspects of Steel I-Girders with Corrugated Steel Webs, *Electronic J. Struct. Engg.*, **7** (2007).
3. J. Moon, J.-W. Yi, B. H. Choi and H.-E. Lee, Shear Strength and Design of Trapezoidally Corrugated Steel Webs, *J. Constructional Steel Res.*, **65**, 1198-1205 (2009).
4. J. Moon, J.-W. Yi, B. H. Choi and H.-E. Lee, Lateral-Torsional Buckling of I-girder with Corrugated Webs Under Uniform Bending, *Thin-Walled Structures*, **47**, 21-30 (2009).
5. G. J. Hancock, Light Gauge Construction, *Progress in Structural Engineering and Materials*, **1(1)**, 25-30 (1997).
6. M. E. A.-H. Eldib, Shear Buckling Strength and Design of Curved Corrugated Steel Webs for Bridges, *J. Constructional Steel Res.*, **65**, 2129-2139 (2009).
7. Y. A. Khalid, C. L. Chan, B. B. Sahari and A. M. S. Hamouda, Bending Behaviour of Corrugated Web Beams, *J. Mater. Proc. Technol.*, **150**, 242-254 (2004).

8. X. Wang, Behavior of Steel Members with Trapezoidally Corrugated Webs and Tubular Flanges under Static Loading, March (2003).
9. M. Elgaaly and A. Seshadri, Depicting the Behaviour of Girders with Corrugated Webs up to Failure using Non-linear Finite Element Analysis, *Adv. Engg. Software*, **29(3-6)**, 195-208 (1998).
10. F. Usman, Shear Buckling of Trapezoidal Web Plate, November (2001).

*Revised : 26.10.2015*

*Accepted : 28.10.2015*